Wave Propagation in Grounded Dielectric Slabs with Double Negative Metamaterials

W. Shu and J. M. Song
Iowa State University, USA

Abstract—In this paper, the wave propagation in a grounded dielectric slab with double negative (DNG) metamaterials is studied. Dramatically different evanescent surface modes (electromagnetic fields exponentially decay both in air and inside the slab) are observed. They are highly dependent on medium parameters. An infinite number of complex surface modes are found to be existing which have proper field distribution in the air region. The investigations on the Poynting vectors show that they do not carry away energy in both transverse and longitudinal directions.

1. Introduction

The guided dielectric slab with a DNG medium has been studied by several groups. Various novel properties are observed: [1] and [2] found that there are special regions for TM (transverse magnetic) modes where two different propagation constants exist. [3] theoretically considered the properties of a planar two-layered waveguide, whose one layer is a double positive (DPS) medium and the other is a DNG medium. Super slowwaves with extremely short wavelengthes were found whose fields exponentially decay from the interface of the two slabs inside both layers. These guided modes, termed as evanescent surface modes, were also found by [4] and [5], respectively. P. Baccarelli and his colleague suggested the concept of surface wave suppression that ensures the absence of both ordinary and evanescent surface modes. This is very attractive in view of taking DNG medium as a potential substrate candidate to reduce edge diffraction effects and enhance radiation efficiency for microstrip antennas [6].

However, so far as the authors are aware no study on the complex modes and Poynting vectors has been reported. This makes the mode spectra of DNG media unpleasantly incomplete. In this paper, the authors focus on the properties of the evanescent surface modes and the complex modes, both of which belong to the proper mode spectra of the grounded dielectric slab with a DNG medium. It is found that the evanescent surface modes are highly dependent on the medium parameters and an infinite number of complex modes exists which have exponentially decaying fields in the air region. They are termed complex surface modes. The study on the Poynting vectors shows that they have zero power flows in both transverse and longitudinal directions.

2. Eigen Equations and Graphical Solutions

The structural setup of interest here is a grounded dielectric slab of thickness d (see Figure 1). Region one is a DNG medium and region two is air. It is well known that to ensure a positive stored energy in the dielectric layer, passive DNG media must be dispersive [7]. However, for simplicity we assume that they are isotropic, losseless, and non-dispersive. This assumption is found to be acceptable since a small dispersion of ϵ and μ can satisfy the constraints.

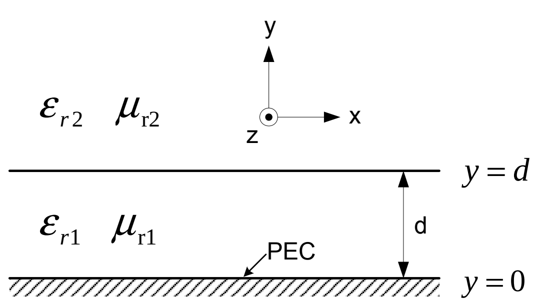

Figure 1: Geometry structure of a grounded dielectric slab with DNG medium ($\epsilon_{r1} < 0, \mu_{r1} < 0$).

Using the well-known transverse resonance method [8], the eigen equations for ordinary ($\gamma_{y1} = jk_{y1}$) real

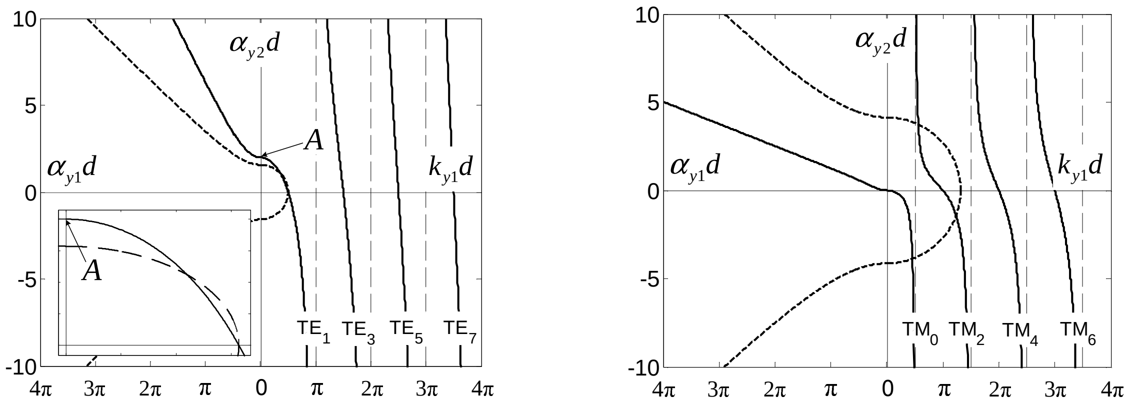

(a) TE (b) TM

Figure 2: Graphical solutions for TE and TM modes. Solid lines in the first and fourth quadrants represent (1) or (2); solid lines in the second quadrant represent (4) or (5); dashed line in the first and fourth quadrants represents (3); dashed line in the second and third quadrants represents (6). The medium parameters are: $\epsilon_{r1} = -2.5, \mu_{r1} = -0.5, \epsilon_{r2} = 1, \mu_{r2} = 1$.

modes are:

$$\frac{\mu_{r2}}{\mu_{r1}}(k_{y1}d)\cot(k_{y1}d) = -\alpha_{y2}d \qquad \text{for TE} \tag{1}$$

$$\frac{\epsilon_{r2}}{\epsilon_{r1}}(k_{y1}d)\tan(k_{y1}d) = \alpha_{y2}d \qquad \text{for TM} \tag{2}$$

$$(k_{y1}d)^2 + (\alpha_{y2}d)^2 = (k_0d)^2(\epsilon_{r1}\mu_{r1} - \epsilon_{r2}\mu_{r2}) \tag{3}$$

The eigen equations for evanescent ($\gamma_{y1} = \alpha_{y1}$) real modes are:

$$\frac{\mu_{r2}}{\mu_{r1}}(\alpha_{y1}d)\coth(\alpha_{y1}d) = -\alpha_{y2}d \qquad \text{for TE} \tag{4}$$

$$\frac{\epsilon_{r2}}{\epsilon_{r1}}(\alpha_{y1}d)\tanh(\alpha_{y1}d) = -\alpha_{y2}d \qquad \text{for TM} \tag{5}$$

$$(\alpha_{y2}d)^2 - (\alpha_{y1}d)^2 = (k_0d)^2(\epsilon_{r1}\mu_{r1} - \epsilon_{r2}\mu_{r2}) \tag{6}$$

where $k_0^2 = \omega^2\mu_0\epsilon_0$. γ_{y1}, γ_{y2} are the y-direction wave constants of the two layers. Their relationship to the longitudinal wave constant (z-direction) γ is written as:

$$\gamma_{yi}^2 = -k_0^2\epsilon_{ri}\mu_{ri} - \gamma^2 \qquad (i = 1, 2) \tag{7}$$

Graphical representations of the above equations are shown in Figure 2. The mode index notation here follows [9]. Notice that in the first and second quadrants, α_{y2} is positive and the fields exponentially decay in the air region (proper); in the third and fourth quadrants, α_{y2} is negative and the fields exponentially increase in the air region (improper). The x-axis is divided into two segments. The right half is for $k_{y1}d$ and the fields in the dielectric layer are sine/cosine standing waves (ordinary), while the left half is for $\alpha_{y1}d$ and the fields in the dielectric layer are exponentially distributed (evanescent). Therefore, the intersection in the second quadrant represents the *proper evanescent* surface mode, which does not exist for a DPS medium.

Another important difference for a DNG medium that can be read from Figure 2 is that the ordinary surface mode solutions are no longer monotonic. It is clear from the subfigure in the left corner of Figure 2(a) that there are two intersections as the radius of the dashed circle decreases, which corresponds to a decrease of frequency. Once the circle has only one tangential point with the solid line, further decreasing frequency will cause this mode to be cutoff. The same thing happens to TM modes in Figure 2(b) in a more obvious way. These two possible modes have two different power flow distributions. One has more power flowing in the air region than in the dielectric region, making the total power flow in the same direction as the phase velocity. The other is in the opposite way and displays a backward property. More details on the Poynting vectors are addressed in Section 4.

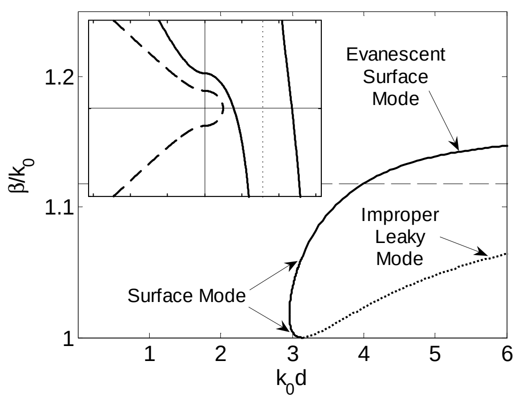

(a) $\epsilon_{r1} = -2.5, \mu_{r1} = -0.5, \epsilon_{r2} = 1, \mu_{r2} = 1$.

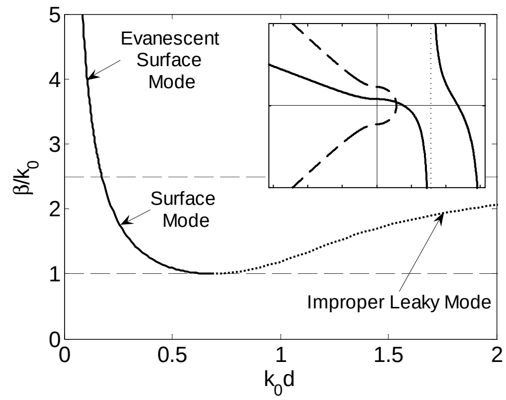

(b) $\epsilon_{r1} = -2.5, \mu_{r1} = -2.5, \epsilon_{r2} = 1, \mu_{r2} = 1$.

Figure 3: Two possible dispersion curves for TE proper surface modes (solid lines) and TE improper leaky modes (dotted lines). The dashed line, representing $\sqrt{\epsilon_{r1}\mu_{r1}}$, is the watershed for evanescent surface mode and ordinary surface modes.

3. Evanescent Surface Mode

As stated in Section 2, the proper evanescent surface mode does exist with a DNG medium. It is the intersection in the second quadrant. The normalized effective dielectric constant $\epsilon_{eff} = (\beta/k_0)^2$ for evanescent surface mode is larger than both $\epsilon_{r1}\mu_{r1}$ and $\epsilon_{r2}\mu_{r2}$. Therefore the transverse propagation constant in the dielectric layer $\gamma_{y1} = \sqrt{-k_0^2\epsilon_{r1}\mu_{r1} - \gamma^2} = k_0\sqrt{\epsilon_{eff} - \epsilon_{r1}\mu_{r1}}$ is a pure real number. The electromagnetic fields are no longer sine/cosine standing waves, but have the form of $Ae^{-\alpha_{y1}y} + Be^{\alpha_{y1}y}$.

It is found, however, that the dispersion curves for evanescent surface modes are very complicated, and they are highly dependent on the medium parameters. Figure 3 shows two dispersion diagrams for TE_1 mode with different medium parameters. The dispersion curves represent the intersection points of the dashed line and the first solid branch in Figure 2(a), including the part in the second quadrant. The solid line in Figure 3 is for proper modes, while the dotted line is for improper mode, which is the set of intersections in the fourth quadrant in Figure 2(a). The dashed lines in both figures depict the value of $\sqrt{\epsilon_{r1}\mu_{r1}}$. They are the watersheds by which one can tell the evanescent surface mode from ordinary ones.

In Figure 3(a), the evanescent surface mode has low cutoff frequency. As the frequency increases, the ordinary surface mode becomes an evanescent surface mode and its effective dielectric constant, ϵ_{eff}, keeps increasing. In Figure 3(b), however, the situation is reversed. The evanescent surface mode has a high cutoff frequency above which it becomes the ordinary surface mode. At the low frequency range, the evanescent surface mode has an extremely large ϵ_{eff}, which decreases rapidly as the frequency increases. One can refer to the subfigures of Figure 3 to check the validations. The reason for such dramatically different dispersion curves is that with DNG metamaterials, one can not only make ϵ and μ simultaneously negative but also let their absolute values be less than one [5]. From (1) and Figure 2(a), it is easy to see that the crossing point of the first solid branch TE_1 with the x-axis is fixed at $(\pi/2, 0)$, while the crossing point with the y-axis noted as 'A' in Figure 2(a) is $(0, |\mu_{r2}/\mu_{r1}|)$. With a conventional DPS medium, μ_{r1} is always equal to unity, or slightly greater or smaller than unity as in the case of paramagnetic or diamagnetic materials. With metamaterials, however, μ_{r1} is not confined near unity any more and the intercept with the y-axis may change a lot. This change affects the possible intersections of the first solid line and the dashed line in Figure 2(a) and finally results in dramatically different dispersion curves.

4. Complex Surface Modes and Poynting Vectors

It is well known that the complete proper mode spectra for a DPS dielectric slab include discrete surface modes and continuous radiation modes, both of which are real modes [8]. With a DNG medium, however, it is proved by the authors that the complex roots of the eigen equations are exclusively on the top Riemann sheet [10]. These solutions, termed complex surface waves, form another set of proper modes since they have exponentially decaying fields in the air region and satisfy the boundary conditions at infinity. Unlike real surface modes, complex surface modes have high cutoff frequencies below which they exist.

Figure 4 shows the dispersion diagrams for both TE and TM modes, including evanescent, ordinary, and

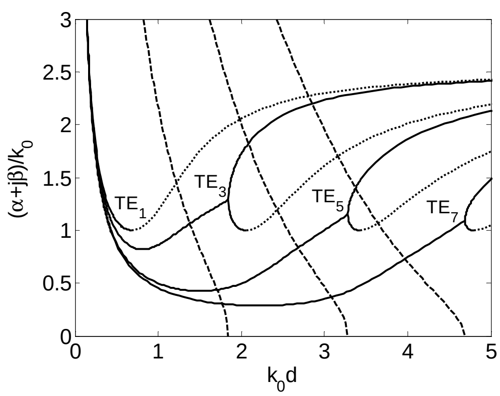

(a) TE

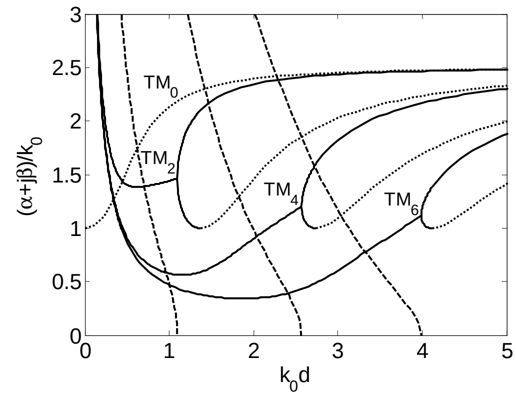

(b) TM

Figure 4: Dispersion diagrams for all modes. Solid line is for normalized β of the proper modes. Dashed line is for normalized α of the proper modes. Dotted line is for normalized β of the improper modes. The medium parameters are: $\epsilon_{r1} = -2.5, \mu_{r1} = -2.5, \epsilon_{r2} = 1, \mu_{r2} = 1$.

complex surface modes. Also included are improper leaky modes drawn as dotted lines. When the frequency is much lower than the first cutoff frequency of the real modes, all complex modes exist with very high normalized α and β. As the frequency increases, β/k_0 tends to decrease rapidly within a very narrow frequency range; after that it increases slowly till its cutoff frequency. Notice it is not monotonic and the value of β/k_0 can be less than unity, which is a notable difference compared with evanescent and ordinary surface modes. The curve of α/k_0, however, monotonically decreases very fast as the frequency increases. At the cutoff point, α reaches zero and β becomes the starting point of the real mode. The real surface mode bifurcates into two branches from this point. One branch has an increasing β/k_0 as the frequency goes high, while the other has a decreasing β/k_0, which will reach unity shortly. This property is expected from Figure 2. Further increasing frequency makes β/k_0 of the second branch begin to rise. However, it is no longer a proper mode.

It is found that the complex surface modes have zero power flows [10]. To derive the Poynting vector for complex modes, γ_{y1}, γ_{y2}, and γ are assumed to be:

$$\begin{aligned} \gamma_{y1} &= a + jb \\ \gamma_{y2} &= u + jv \\ \gamma &= \alpha + j\beta \end{aligned} \tag{8}$$

The Poynting vector is written as

$$S_z^{\mathrm{TE}} = \frac{1}{2} E_x H_y^* = \frac{|A|^2}{2} \begin{cases} S_{z1}^{\mathrm{TE}}, & \text{for } 0 < y < d \\ S_{z2}^{\mathrm{TE}}, & \text{for } y \geq d \end{cases} \tag{9}$$

where A is the electric field intensity and S_{z1}^{TE} and S_{z2}^{TE} are as follows:

$$S_{z1}^{\mathrm{TE}}(y,z) = \frac{\beta + j\alpha}{2\omega\mu_{r1}} e^{-2\alpha z} [\cosh(2ay) - \cos(2by)] \tag{10}$$

$$S_{z2}^{\mathrm{TE}}(y,z) = \frac{\beta + j\alpha}{2\omega\mu_{r2}} e^{-2u(y-d)-2\alpha z} [\cosh(2ad) - \cos(2bd)] \tag{11}$$

Figure 5 shows the dispersion diagram and the integral results of Poynting vector for the TE_3 mode. In Figure 5(a), only the complex mode exists (branch 'A') when the frequency is lower than the cutoff frequency of the real surface mode. The zero power flow in z-direction in Figure 5(b) shows that the complex surface mode does not carry away any energy. As the frequency increases, the real surface mode begins. The top branch (branch 'B') of the real mode carries a negative power flow and shows backward properties. When a waveguide operates in this mode, its fields are largely confined inside the dielectric layer. The bottom branch (branch 'C') of the real mode carries a positive power flow and its fields extend far away in the air region. Further increasing frequency causes the fields in the air region to decay more slowly, and eventually reach infinity. At that point, the radiation boundary conditions are violated and the mode becomes improper.

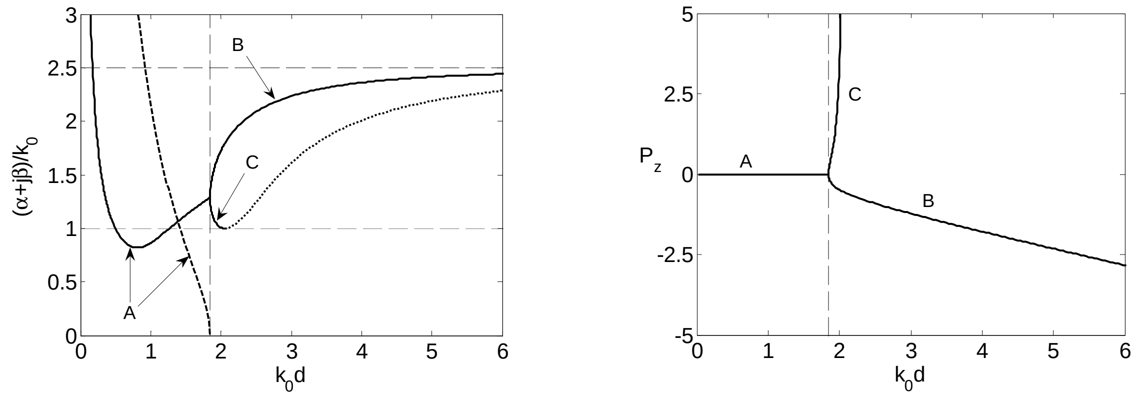

(a) Dispersion diagram (b) Power flow in z-direction

Figure 5: Dispersion diagram and the power flow in z-direction for TE modes. 'A' is for complex surface mode; 'B' is for top branch of the real surface mode; 'C' is for bottom branch of the real surface mode. The medium parameters are: $\epsilon_{r1} = -2.5, \mu_{r1} = -2.5, \epsilon_{r2} = 1, \mu_{r2} = 1$.

5. Conclusion

In this paper, an investigation on the mode properties of a grounded dielectric slab with a DNG medium has been dealt with. The graphical method is used to find the possible real roots. Dramatically different dispersion curves of evanescent surface modes are observed, showing that they are very sensitive to the material parameters. It is found that there is an infinite number of complex surface modes with a DNG medium and they do not carry away energy. Although the considered medium here is idealized and currently cannot be realized, the results of this paper still unveil some exotic properties as well as potential applications of the metamaterials.

REFERENCES

1. Cory, H. and A. Barger, "Surface-wave propagation along a metamaterial slab," *Microwave Opt. Technol. Lett.*, Vol. 38, 392–395, Sept. 2003.
2. Dong, H. and T. X. Wu, "Analysis of discontinuities in double-negative (DNG) slab waveguides," *Microwave Opt. Technol. Lett.*, Vol. 39, 483–488, Dec. 2003.
3. Nefedov, I. S. and S. A. TretyaKov, "Waveguide containing a backward-wave slab," *Radio Sci.*, Vol. 38, 1101–1109, 2003.
4. Wu, B.-I., T. M. Grzegorczyk, Y. Zhang, and J. A. Kong, "Guided modes with imaginary transverse wave number in a slab waveguide with negative permittivity and permeability," *J. Appl. Phys.*, Vol. 93, 9386–9388, Jun. 2003.
5. Shadrivov, I. W., A. A. Sukhorukov, and Y. S. Kivshar, "Guided modes in negative-refractive-index waveguides," *Phys. Rev. E, Stat. Phys. Plasmas Fluids Relat. Interdiscip. Top.*, Vol. 67, 057602–057602, May 2003.
6. Baccarelli, P., P. Burghignoli, F. Frezza, A. Galli, P. Lampariello, G. Lovat, and S. Paulotto, "Fundamental modal properties of surface waves on metamaterial grounded slabs," *IEEE Trans. Microwave Theory Tech.*, Vol. 53, 1431–1442, Apr. 2005.
7. Smith, D. R. and N. Kroll, "Negative refractive index in left-handed materials," *Phys. Rev. Lett.*, Vol. 85, 2933–2936, Oct. 2000.
8. Collin, R. E., *Field Theory of Guided Waves*, 2nd, Ed. Piscataway, IEEE Press, NJ, 1991.
9. Balanis, C. A., *Advanced Engineering Electromagnetics*, John Wiley & Sons, NJ, 1989.
10. Shu, W. and J. M. Song, "On the properties of a grounded dielectric slab with double negative metamaterials," *IEEE Trans. Microwave Theory Tech.*, to be submitted.